NJC

ROYAL SOCIETY OF CHEMISTRY

PAPER

View Article Online
View Journal | View Issue

Cite this: *New J. Chem.*, 2022, **46**, 21221

Role of ligand spacer length of a tripodal amide on uranium(VI) and plutonium(IV) complexation: synthesis, solvent extraction, liquid membrane transport and theoretical studies†

Ananda Karak,[ab] Bholanath Mahanty,[c] Prasanta K. Mohapatra,*[bc] Sk. Musharaf Ali,[d] Richard J. M. Egberink,[e] Darshan B. Sathe,[a] Raj B. Bhatt,[a] Thisur P. Valsala,[a] Jurriaan Huskens[e] and Willem Verboom*[e]

Liquid–liquid extraction of several actinide and lanthanide ions, *viz.*, U(VI), Pu(IV), Am(III) and Eu(III) was investigated from nitric acid feed solutions employing *N*,*N*,*N*′,*N*′,*N*″,*N*″-hexa-*n*-octyl nitrilotripropamide (HONTP) in 90% *n*-dodecane + 10% isodecanol. The observed trend of metal ion extraction at 0.5 M HNO_3 was Pu(IV) > U(VI) > Eu(III) ~ Am(III). A high distribution ratio was observed for U(VI) at pH 2 using 0.08 M HONTP in 90% *n*-dodecane + 10% isodecanol. The back extraction study of Pu(IV) and U(VI) using 0.5 M HNO_3 + 0.5 M oxalic acid and 1 M Na_2CO_3, respectively, showed highly efficient stripping (>97%) for both the metal ions from the loaded organic phase. Slope analysis suggested formation of a lower stoichiometry complex of Pu(IV) with HONTP at 3 M HNO_3, whereas U(VI) formed 1 : 1 (ML) and 1 : 2 (ML_2) species. Temperature variation studies on the extraction of the metal ions showed that complexation of U(VI) with HONTP was not favourable, based on entropy changes. A supported liquid membrane study showed very poor transport of U(VI) using 0.08 M HONTP in 90% *n*-dodecane + 10% isodecanol, whereas Pu(IV) exhibited significant transport through the membrane. Density functional theoretical (DFT) studies were carried out to corroborate the experimental observations. Comparison of the results with those of hexa-*n*-octyl nitrilotriacetamide (HONTA) revealed a considerable effect of the spacer length on the binding efficiency, selectivity, and complex stoichiometry.

Received 7th July 2022,
Accepted 20th October 2022

DOI: 10.1039/d2nj03354b

rsc.li/njc

Introduction

In view of the ever-increasing energy demands, the growth of nuclear power production is increasing very rapidly in the last few decades and it is considered as a viable alternative to the conventional energy resources. However, one of the major challenges in the global acceptance of nuclear energy is the safe management of the hazardous radioactive waste materials emanating at various stages of the nuclear fuel cycle operations. In a closed fuel cycle, the separation of actinides such as U and Pu is being done by the well known PUREX (Plutonium Uranium Redox Extraction) process which uses TBP (tri-*n*-butyl phosphate) in a paraffinic hydrocarbon as the solvent.[1] Due to the deleterious nature of the degradation products of TBP, alternative 'green' solvents based on dialkyl monoamides have been proposed based on their favourable extraction behaviour.[2–7] Subsequently, a variety of dialkyl monoamides are being used for the extraction of UO_2^{2+} and Pu(IV) from nitric acid medium, some of them showing very good selectivity towards the hexavalent actinide ions such as UO_2^{2+} with respect to Pu(IV).[8,9] Recent studies have indicated that ligands containing multiple amide groups are highly efficient in metal ion extraction as seen with the tripodal amides.[10,11] We have studied different alkyl derivatives of hexa-*n*-alkyl nitrilotriacetamide (HRNTA) ligands where three acetamide groups are attached to the central pivotal nitrogen atom to form tripodal amide ligands (Fig. 1a). They display promising results for the extraction of Pu(IV) ions as compared to that of UO_2^{2+} and Am(III) ions from nitric acid feed solutions.[12–15] Out of the different alkyl NTA ligands (alkyl: *n*-butyl, *n*-hexyl, *n*-octyl and

[a] *INRPO, FF, Nuclear Recycle Board, Bhabha Atomic Research Centre, Tarapur, India*
[b] *Homi Bhabha National Institute, Anushakti Nagar, Mumbai-400094, India*
[c] *Radiochemistry Division, Bhabha Atomic Research Centre, Mumbai-400085, India. E-mail: mpatra@barc.gov.in*
[d] *Chemical Engineering Division, Bhabha Atomic Research Centre, Mumbai-400085, India*
[e] *Laboratory of Molecular Nanofabrication, Department for Molecules & Materials, MESA+ Institute, University of Twente, P.O. Box 217, 7500 AE Enschede, The Netherlands. E-mail: w.verboom@utwente.nl*

† Electronic supplementary information (ESI) available. See DOI: https://doi.org/10.1039/d2nj03354b

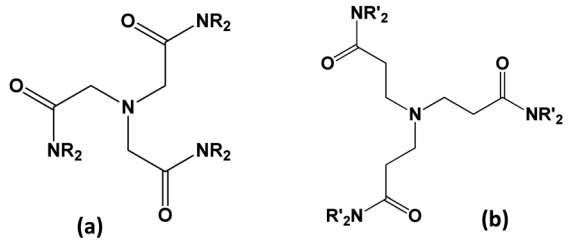

R = *n*-C_4H_9, *n*-C_6H_{13}, *n*-C_8H_{17} (HONTA)

R′ = *n*-C_8H_{17}

Fig. 1 Structural formula of (a) *N,N,N′,N′,N″,N″*-hexa-*n*-alkylnitrilotriacetamide (HRNTA), (b) *N,N,N′,N′,N″,N″*-hexa-*n*-octylnitrilotripropamide (HONTP).

n-dodecyl) studied by us, the hexa-*n*-octyl nitrilotriacetamide (HONTA) ligand was found to be superior for the extraction of tetravalent metal ions from nitric acid medium. However, the spacer length effect of the HRNTA ligands is unexplored. In view of this, the present work deals with the synthesis and evaluation of a HONTA homolog with an ethylene spacer (HONTA has methylene spacers). Hexa-*n*-octyl nitrilotripropanamide (HONTP) (Fig. 1b) was investigated for the extraction of different actinide ions from aqueous nitric acid medium. Apart from the solvent extraction studies, we have also carried out liquid membrane transport studies[16,17] and density functional theoretical (DFT) studies.[18]

Results and discussion

Solvent extraction studies

Extraction and stripping kinetics. To ensure effective metal ion extraction, it is necessary to study the time of equilibration so that the obtained *D*-values reach to a maximum value. For this reason, the extraction of Pu(IV), U(VI) and Am(III) using 0.08 M HONTP in 90% *n*-dodecane + 10% isodecanol was studied (Fig. S1, ESI†). The extraction kinetics data suggest fast extraction kinetics (within 10 minutes) for all the metal ions studied here (details are given in the ESI†).

Similarly, to recycle the extractant solution, stripping of the loaded metal ions should be facile so that a sustainable process can be developed. Stripping of Pu(IV) and U(VI) ions from the loaded organic phases containing HONTP in 90% *n*-dodecane + 10% isodecanol was carried out using 0.5 M oxalic acid + 0.5 M HNO_3 and 1 M Na_2CO_3, respectively.[9,11] The stripping kinetics with both metal ions was fast and within 10 minutes it reaches equilibrium *D*-values. Using the respective stripping solutions for Pu(IV) and U(VI) more than 97% and 99% metal ions can be stripped from their corresponding organic phase, respectively.

Extraction of actinide metal ions. Extraction of actinide and lanthanide ions *viz.*, Pu(IV), U(VI), Eu(III) and Am(III) was carried out at 0.5 M nitric acid solution using 0.08 M HONTP in 90% *n*-dodecane + 10% isodecanol. The observed trend of the metal ion extraction (shown in Table 1) being: Pu(IV) > U(VI) >> Eu(III) ~ Am(III). This may be explained in terms of decreasing ionic potential values (or the residual charge on the metal in case of the uranyl ion) of the metal ions as Pu(IV) > U(VI) > Eu(III) ~ Am(III).[19,20] The extraction of the trivalent lanthanide/actinide ions was negligible (Table 1).

Table 1 Extraction at 0.5 M HNO_3 with 0.08 M HONTP in 90% *n*-dodecane + 10% isodecanol

Metal ion	D_M	Ionic radius[a] (Å)
U(VI)	0.019 ± 0.001	0.86
Pu(IV)	0.580 ± 0.029	0.96
Eu(III)	$<2.0 \times 10^{-4}$	1.066
Am(III)	$<1.0 \times 10^{-4}$	1.09

[a] Ref. 21.

Effect of nitric acid concentration on metal ion extractions

The extraction of metal ions by neutral donor ligands such as the tripodal HONTP used in the present study can be given by the following extraction equilibrium:

$$M^{n+}_{aq} + nNO_{3aq}^{-} + yA_{org} \overset{K_{ex}}{\rightleftharpoons} M(NO_3)_n \cdot yA_{org} \quad (1)$$

According to eqn (1), the metal ions form their respective extractable metal–ligand complex after binding with '*n*' number of nitrate ions to get charge neutrality of the complex and '*y*' number of ligand molecules to yield a hydrophobic complex.

In the liquid–liquid extraction studies, it was observed that the distribution ratio (*D*) value (it is the ratio of concentration of metal ion in the organic phase to that in the aqueous phase, details given in the ESI†) of the metal ions changed with increasing nitric acid concentration in the aqueous phase. In the present study, the effect of the feed acid concentration on the distribution ratio was investigated for Pu(IV), U(VI), Am(III) and Eu(III) using 0.08 M HONTP in 90% *n*-dodecane + 10% isodecanol (Fig. 2a).

The *D*-value of Pu(IV) extraction was found to increase from 0.5 M to 6 M. Fig. 2a shows that the *D*-value was 0.58 at 0.5 M HNO_3 which increased to >3 at 6 M HNO_3. This is due to nitrate ion participation in the complex formation as clearly seen from eqn (1). The *D*-value for U(VI) extraction decreased sharply going from 0.01 M to 0.1 M nitric acid, beyond which a near constant *D*-value was observed followed by a gradual increase in the concentration range of 0.5 M to 6 M. The high *D*-value of U(VI) at 0.01 M nitric acid may be explained as participation of two ligand molecules (HONTP) (*vide infra*) in the extracted complex species with a concomitant enhanced lipophilicity of the metal–ligand complex. Apparently, the flexibility of HONTP facilitates the positioning of the amide groups around the UO_2^{2+} ion in a favourable topology. With increase in the nitric acid concentration from 0.01 M to 0.5 M, there is a possibility of protonation at the central nitrogen atom of the ligand resulting in a decrease in the free ligand availability, which may be the reason for the decrease in the distribution ratio values. The gradual increase in the *D*-values from 0.5 M to 6 M nitric acid may be caused by an increased tendency of

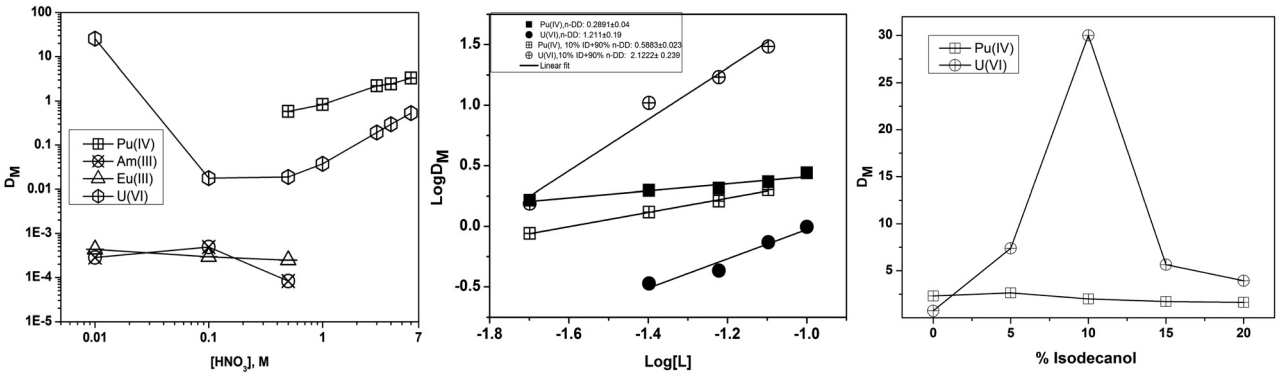

Fig. 2 (a) Effect of nitric acid on the *D*-value of actinide metal ions; 0.08 M HONTP in 90% *n*-dodecane + 10% isodecanol; (b) dependence of *D*-value of Pu(IV) and U(VI) with ligand concentration; aqueous phase: 3.0 M and 0.01 M HNO_3 for Pu(IV) and U(VI), respectively; organic phase: *x* M HONTP in 90% *n*-dodecane + 10% isodecanol; (c) effect of isodecanol content on the distribution ratio of U(VI) and Pu(IV) at 0.01 M and 3 M HNO_3, respectively; organic phase: 0.08 M HONTP in *n*-dodecane + isodecanol.

complex formation due to the availability of more nitrate ions (eqn (1)) and to a better salting out effect. The very low *D*-values of Am(III) and Eu(III) in 0.01 M to 0.5 M HNO_3 may be due to the lower ionic potential values of Am(III) and Eu(III) (Table 1).

Nature of the extracted species. It is important to determine the stoichiometry of the metal–ligand complex which can explain its extractability into the organic phase. The distribution ratio (D_M) and the extraction equilibrium constant (K_{ex}) in the two-phase extraction system (according to eqn (1)) can be related with eqn (2) (details are given in ESI†):

$$\log D_M = \log K_{ex} + n \log[NO_3^-]_{aq} + y \log[L]_{org} \qquad (2)$$

where [L] is the ligand concentration in the organic phase. The stoichiometry of the complexes of HONTP with U(VI) and Pu(IV) was determined from slope analysis of the respective log–log plots of the distribution ratio values (D_M) *vs.* HONTP concentrations (Fig. 2b) at a fixed nitrate ion concentration. Since the metal ion concentrations are taken at tracer level compared to the extractant concentrations in these studies, the concentration of the free ligands can be considered to be the same as its initial concentration.

U(VI) extraction was studied at varying ligand concentrations using both HONTP in *n*-dodecane and in 90% *n*-dodecane + 10% isodecanol at 0.01 M HNO_3 and the slope values of the log–log plots were 1.21 ± 0.19 and 2.12 ± 0.24, respectively. This indicates that HONTP forms ML species during U(VI) extraction into *n*-dodecane and ML_2 species during the corresponding extraction into 90% *n*-dodecane + 10% isodecanol. Similarly, the corresponding Pu(IV) extraction performed at 3 M HNO_3 resulting in slope values of 0.29 ± 0.04 and 0.59 ± 0.02, respectively.

This shows that the stoichiometry of the metal–ligand complex is affected by the modified composition of the organic medium. Isodecanol plays a significant role in changing the stoichiometry of the metal–ligand complex through its interaction with the extractant molecules. Therefore, we have carried out some studies at varying concentrations of isodecanol and the results are discussed below (*vide infra*).

Effect of isodecanol on extraction

In liquid–liquid extraction, isodecanol is being used in the organic phase as a modifier to minimize third-phase formation by increasing the polarity of the organic medium.[22] Extraction of U(VI) and Pu(IV) was carried out using 0.08 M HONTP with varying isodecanol content in the organic phase containing *n*-dodecane. It was found that the *D*-values of U(VI) increased very sharply till attaining a maximum value at 10% isodecanol, beyond which there was a decreasing trend (Fig. 2c).

For Pu(IV), the changes in the metal ion extraction are much sober with varying isodecanol content (Fig. 2c). Isodecanol may interact with the ligand and molecules of the former may disperse the HONTP molecules to interact more to the metal ion rather than to themselves, thereby increasing the *D*-value initially with isodecanol content. However, at higher isodecanol concentration, there is more interaction of isodecanol with the ligand molecules, which may decrease the reactivity of HONTP towards metal ion binding.[22,23]

Influence of temperature on metal ion extraction. The influence of temperature on the extraction of U(VI) and Pu(IV) was investigated in the range of 15 °C to 45 °C using 0.08 M HONTP in *n*-dodecane/90% *n*-dodecane + 10% isodecanol mixture. The details of the extraction study are given in the ESI.† The different thermodynamic parameters determined from the temperature variation study are included in Table 2.

The data in Table 2 indicate that the extraction of U(VI) by the ligand is enthalpy driven, whereas that of Pu(IV) is entropy driven. Pathak *et al.* reported that U(VI) extraction by ligands with sterically hindered alkyl groups like D2EHIBA (di-2-ethylhexyl isobutyramide) and D2EHPVA (di-2-ethylhexylpivalamide) is more enthalpy favoured than other ligands.[24] The positive entropy change with the Pu(IV) complexation may be due to the formation of a less associated metal–ligand species as also evident from the ligand concentration variation experiment (*vide supra*) and also to more release of the water molecules during complexation. The negative entropy change with the extraction U(VI) may be due to more associated metal–ligand species formation (M : L as 1 : 1 or 1 : 2) and also to a lesser release of the water molecules. The

Table 2 Thermodynamic parameters of the metal–HONTP complex in the extraction with 0.08 M HONTP in different diluents

Metal ions	D_M	$\log K_{ex}$	ΔG (kJ mol^{-1})	ΔH (kJ mol^{-1})	ΔS (kJ mol^{-1} K^{-1})
UO_2^{2+} [a]	30.0 ± 0.2	7.75	−44.2	−126.5	−0.28
Pu^{4+} [a]	2.0 ± 0.1	1.45	−5.15	7.4	0.04
UO_2^{2+} [b]	0.739 ± 0.001	5.05	−28.8	−56.5	−0.09

[a] 90% *n*-Dodecane + 10% isodecanol. [b] *n*-Dodecane.

entropy change trend is also supported by theoretical studies (*vide infra*).

Effect of absorbed dose on extraction. For the successful recycling of the extractant, a study of the radiolytic stability of the extractant is very important. A solution of 0.08 M HONTP in 90% *n*-dodecane + 10% isodecanol was irradiated in a gamma chamber (^{60}Co gamma rays) and the total absorbed dose on the sample was 320 kGy. Extraction of Pu(IV) and U(VI) was carried out using the irradiated HONTP solution and the results are presented in Table 3. The *D*-values of U(VI) decreased quite significantly after irradiation, whereas there is a marginal decrease in the D_{Pu}-ratio. This may be due to the formation of degradation products which have a similar or lower tendency for Pu(IV) extraction. However, a marginal increase in the *D*-values of Pu(IV) was observed in our earlier work with HONTA on irradiation with gamma rays.[14] Gujar *et al.* also reported an increase in the *D*-value for Pu(IV) extraction with TREN-DGA (a substituted tripodal diglycolamide ligand).[25]

Supported liquid membrane studies. The extraction and stripping kinetics of Pu(IV) and U(VI) in 0.08 M HONTP in 90% *n*-dodecane + 10% isodecanol appeared to be fast (within 10 minutes; ESI†). This encouraged us to study the facilitated transport of Pu(IV) and U(VI) ions across PTFE flat sheets containing 0.08 M HONTP in 90% *n*-dodecane + 10% isodecanol in the pores.

The stripping agents used in the receiver compartment were 0.5 M oxalic acid + 0.5 M HNO_3 and 1 M Na_2CO_3 for Pu(IV) and U(VI), respectively (*vide supra*). It was found that 47.2% of Pu(IV) was transported through the membrane in 4 h of continuous operation (Fig. 3) using 3 M nitric acid as the feed solution, which increased to 99% after 24 h. Similarly, there was only 7.0% U(VI) transport in 4 h with 0.01 M HNO_3 as the feed solution, which increased to only 8.5% after 24 h. The U(VI) content in the feed solution decreased from 100% to 48.9% after 24 h in the feed phase, while the mass transport was not quantitative into the receiver phase. The decreased U(VI) amount was found to be retained in the membrane phase.

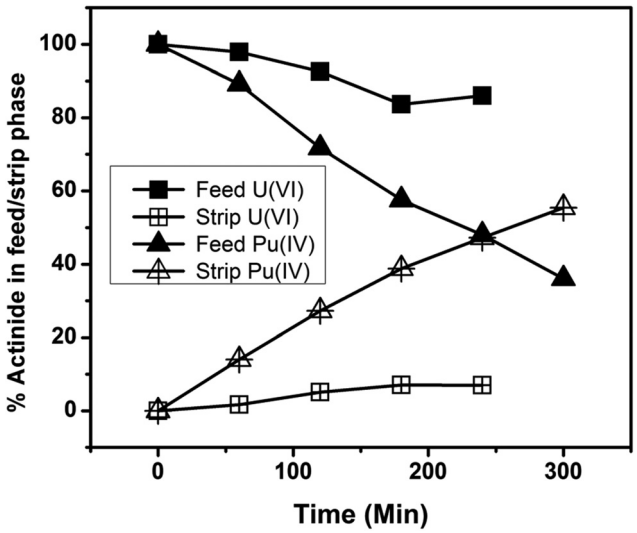

Fig. 3 Transport of U(VI) and Pu(IV) across a PTFE flat sheet SLM with HONTP as carrier ligand in 90% *n*-dodecane + 10% isodecanol); empty symbol: strip phase, filled symbol: feed phase.

In the liquid–liquid extraction study, mentioned above, the distribution ratio value of U(VI) was around 30 at pH 2 using 0.08 M HONTP in 90% *n*-dodecane + 10% isodecanol, the stoichiometry of the metal–ligand complex being 1 : 2. Therefore, it is speculated that there may be hindrance in the transport of the metal–carrier complex through the membrane phase due to its larger size and this could be the reason for the poor transport of uranium. On the other hand, though the D_{Pu} was 2.0, the lower metal–ligand stoichiometry (*vide supra*) at 3 M HNO_3 led to species with lower molar volume and hence, lesser resistance for mass transport in the membrane phase. The stability of the membrane was studied by evaluating the transport efficiency for five different cycles over a period of 12 days and it was found that the *P* (permeability coefficient)-values were nearly constant till the 8th day (Table S1, ESI†).

Comparative study with HONTA. Though HONTP has binding sites similar to that of HONTA (Fig. 1), the former has ethylene spacers in its structure which led to completely different distribution ratios of actinides and selectivities. U(VI), Pu(IV) and Am(III) showed lower distribution ratios at 0.5 M HNO_3 with HONTP compared to those with HONTA[14] (Table 4). Also, the extraction trend reversed for U(VI) and Am(III) extraction.

Interesting observations were made during the extraction studies carried out at pH 2. U(VI) and Am(III) showed *D*-values of 30 and 0.0003, respectively, using 0.08 M HONTP in 90% *n*-dodecane + 10% isodecanol., whereas the corresponding

Table 3 Effect of radiation on distribution ratios of U(VI) and Pu(IV); organic phase: 0.08 M HONTP in 90% *n*-dodecane + 10% isodecanol

Metal ion	[HNO_3] (M)	$D_{M,HONTP}$ 0 kGy	$D_{M,HONTP}$ 320 kGy
U(VI)	0.01	30.0	0.89
Pu(IV)	3	2.0	1.42

Table 4 Distribution ratios of metal ions at 0.5 M HNO_3; organic phase: 0.08 M HONTA/HONTP in 90% *n*-dodecane + 10% isodecanol

Metal ion	$D_{M,HONTA}$	$D_{M,HONTP}$
U(VI)	0.043	0.018
Pu(IV)	124.2	0.58
Am(III)	0.267	<0.0001

values were 0.072 and 3.36, respectively, using 0.02 M HONTA in the same diluent. The lower distribution ratio values of Am(III) and Pu(IV) with HONTP may be attributed to the longer chain arms of the amide groups tethered to the central *N*-atom which cannot effectively bind with the relatively smaller sized metal ions (Am(III) and Pu(IV)), whereas the bigger size UO_2^{2+} ion can be suitably fitted in the tripodal HONTP ligand (Table 4).

SLM studies for U(VI) and Pu(IV) were carried out using 0.08 M HONTA/HONTP in 90% *n*-dodecane + 10% isodecanol in the membrane pores, while the stripping solutions used were 1 M Na_2CO_3 and 0.5 M oxalic acid + 0.5 M HNO_3, respectively. After 4 h of continuous operations, the U(VI) transport at pH 2 feed solution was <1% and 7% for HONTA and HONTP, respectively, whereas the Pu(IV) transport was 78.2% and 47.2% using HONTA[15] and HONTP, respectively, at 3 M HNO_3 as the feed solution (Table 5). Very poor transport of U(VI), in spite of the high *D*-value, in HONTP was due to poor diffusional transport through the membrane. The lower *P*-value due to the *D*-value of Pu(IV) in HONTP resulted in a reduced transport rate of Pu(IV).

A significant change in the stoichiometry of the metal–ligand complexes (shown in Table 6) was observed with HONTP and HONTA in 90% *n*-dodecane + 10% isodecanol for U(VI) and Pu(IV). Due to the presence of the ethylene spacer in HONTP, its binding efficiency with the metal ions and the types of interactions differs from that of HONTA having a methylene spacer.

ATR-FTIR studies. ATR-FTIR studies were carried out with the extracted phases of U(VI) with HONTA and HONTP at pH 2.0 (Fig. S4a, ESI†). The FTIR data indicate two peaks at 1601 cm^{-1} and 1650 cm^{-1} with the extracted HONTP phase, and a single peak at 1639 cm^{-1} with the extracted HONTA phase corresponding to a carbonyl stretching frequency band. We found very poor extraction of U(VI) with HONTA and high extraction of U(VI) with HONTP at pH 2.0 with 0.08 M ligand in 90% *n*-dodecane + 10% isodecanol. The peak at 1601 cm^{-1} in case of the HONTP extract is due to the weakening of the >C=O stretching frequency due to the bonding with the uranyl ion, while the peak at 1650 cm^{-1} corresponds to the free carbonyl (not complexed with the uranyl ion). Such a significant shift points to strong complexation with the uranyl ion by the HONTP ligand. Similarly, a single peak at 1639 cm^{-1} with HONTA indicates the poor extraction of U(VI) at pH 2.0. Moreover, the FTIR spectra also showed the presence of two peaks at 1275 cm^{-1} and 1303 cm^{-1} with HONTP extract which corresponds to the O–N–O symmetric and asymmetric stretching wave number respectively (Fig. S4b, ESI†). The difference in the O–N–O symmetric and asymmetric stretching wave number can be used to ascertain the mode of nitrate ion binding with the metal ion. If the difference is greater than 186 cm^{-1}, it indicates bi-dentate coordination whereas lower than 115 cm^{-1} shows mono-dentate coordination by the nitrate ion.[26] For the present HONTP system, the difference was found to be 28 cm^{-1} which indicates mono dentate coordination by the nitrate ion. This is also supported by the theoretical studies (*vide infra*). In case of HONTA extract, poor extraction of U(VI) into the organic phase lead to no peak splitting at 1303 cm^{-1} and it probably corresponds to the O–N–O asymmetric stretching of HONTA HNO_3 adduct.

Table 5 Percentage transport and permeability coefficient (*P*) of Pu(IV); Membrane: PTFE filled in 0.08 M HONTA/HONTP in 90% *n*-dodecane + 10% isodecanol; feed: 3 M HNO_3, strippant: 0.5 M HNO_3 + 0.5 M oxalic acid, data at 4 h

Ligand	% Transport	$P_{Pu(IV)} \times 10^3$ (cm s^{-1})
HONTP	47.2	0.38 ± 0.01
HONTA	78.2	0.70 ± 0.04

Table 6 Slope values obtained in the ligand concentration variation with HONTA and HONTP in 90% *n*-dodecane + 10% isodecanol with different metal ions. Aqueous phase: U(VI) at pH 2.0 and Pu(IV) at 3 M HNO_3

Ligand	U(VI)	Pu(IV)
HONTA	1.11 ± 0.04	1.84 ± 0.06
HONTP	2.12 ± 0.24	0.59 ± 0.02

Computational studies

Structural parameters. The minimum energy structures of free HONTA and HONTP molecules are displayed in Fig. 4a and b, whereas the complexes of Pu^{4+} and UO_2^{2+} ions towards HONTA/HONTP in presence of nitrate ions are displayed in Fig. 4c–f. The calculated structural parameters for these complexes are presented in Table 7. In both the complexes of the Pu^{4+} ion (1:2 stoichiometry with HONTA and 1:1 with HONTP), the first sphere of the coordination number (CN) was found to be nine (five coordinated sites from two ligands and four coordinated sites from four monodentate nitrate ions for 1:2 stoichiometry. One donor O atom from one ligand points away from the central Pu ion). In case of 1:1 stoichiometry, two O donors from two monodentate nitrates, four O donors from two bidentate nitrates and three O donors from one HONTP unit lead to nona-coordination to the central Pu^{4+} ion. In the 1:1 complex of UO_2^{2+} with HONTA, the central uranyl ion is coordinated to two nitrate anions in monodentate mode and two O donors from one unit of HONTA leading to tetra-coordination. However, with HONTP (1:2), the central uranyl ion is coordinated to two nitrate anions in monodentate mode and three O donors from two HONTP units leading to penta-coordination. The >C=O bond length of free HONTA and HONTP is slightly elongated upon complex formation with Pu and uranyl metal ions. The average Pu–O bond distance (>C=O) in [$Pu(NO_3)_4$–$HONTA_2$] is 2.5505 Å, whereas it is 2.357 Å in [$Pu(NO_3)_4$–HONTP]. The average Pu–O bond distance (–NO_3) in [$Pu(NO_3)_4$–$HONTA_2$] is 2.323 Å, whereas it is 2.370 Å in [$Pu(NO_3)_4$–HONTP]. Point to be noted, the metal oxygen bond distance with the nitrate O is shorter than that of the O atoms of >C=O for the Pu metal ion.

Thermodynamical free energy of complexation. The Gibbs free energy of complexation for Pu^{4+} and UO_2^{2+} ions with both the ligands in the solution phase is presented in Table S2, ESI.† The explicit hydration of Pu^{4+} and UO_2^{2+} ions with 10 and 5 water molecules, respectively, in the first solvation shell was

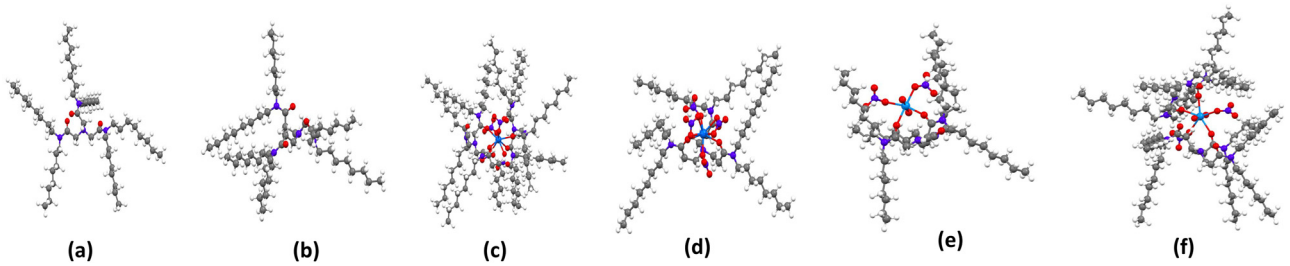

Fig. 4 Optimized structure of (a) HONTA; (b) HONTP; (c) Pu^{4+}–HONTA; (d) Pu^{4+}–HONTP; (e) UO_2^{2+}–HONTA and (f) UO_2^{2+}–HONTP. The grey and white spheres correspond to C and H atoms, whereas red and blue ones denote O and N atoms and cyan spheres represent Pu or U atoms (expanded view of Fig. 4 is shown in Fig. S6, ESI†).

Table 7 Calculated values of bond length (Å) in the gas phase for the various chemical species

Chemical species	C═O	M–O (C═O)	M–O(NO_3)
HONTA	1.220, 1.224, 1.228		
HONTP	1.220, 1.224, 1.228		
$Pu(NO_3)_4$–$(HONTA)_2$	1.232, 1.242, 1.254, 1.232, 1.236, 1.238	2.468, 2.451, 2.805, 2.367, 2.435	2.313, 2.345, 2.295, 2.340
$Pu(NO_3)_4$–(HONTP)	1.230, 1.251, 1.255	2.354, 2.361, 3.948	2.253, 2.264, 2.418, 2.438, 2.402, 2.445
$UO_2(NO_3)_2$–HONTA	1.230, 1.243, 1.248	2.338, 2.407, 4.647	2.267, 2.303
$UO_2(NO_3)_2$–$(HONTP)_2$	1.223, 1.227, 1.249, 1.231, 1.246, 1.249	2.423, 2.468, 2.454, 5.425, 6.392, 6.802	2.316, 2.423

considered for evaluating the complexation free energy. The entropy of complexation was found to be positive in all cases, except for the 1 : 2 complex of uranyl ion with HONTP. HONTP displayed a higher Gibbs free energy of complexation for Pu^{4+} ion in 1 : 1 stoichiometry.

Bonding analysis. In order to get insight into the nature of bonding in the complexes of the Pu^{4+} and UO_2^{2+} ions with HONTP, the charge on the metal ions and the atomic orbital population in the complexes was analyzed using the method of natural population analysis (NPA).[27,28] The calculated values are presented in Table S2, ESI.† The substantial positive charge on the Pu^{4+} and UO_2^{2+} ions points to an ion–dipole type of interaction.

Conclusions

The present study involves the liquid–liquid extraction of U(VI), Pu(IV), Am(III) and Eu(III) using 0.08 M HONTP in 90% *n*-dodecane + 10% isodecanol. At 0.5 M HNO_3 the observed extraction trend was Pu(IV) > U(VI) > Eu(III) ∼ Am(III). U(VI) shows a high distribution ratio at pH 2, whereas Am(III) shows very poor extraction. Extraction and stripping kinetics were completed within 10 minutes for U(VI) and Pu(IV). Pu(IV) forms lower stoichiometric complexes with HONTP at 3 M HNO_3, whereas the stoichiometry of the U(VI)–ligand complex depends on the polarity of the organic phase. U(VI) forms 1 : 2 (ML_2) and 1 : 1 (ML) species in 90% *n*-dodecane + 10% isodecanol and in *n*-dodecane, respectively, at pH 2. Irradiation with 320 kGy gamma ray gives rise to significant changes in the *D*-values of U(VI) and Pu(IV). In SLM studies with HONTP, Pu(IV) transport was 47.2% at 4 h operation using 3 M feed solution, whereas U(VI) transport was only 7% using 0.01 M feed solution. The DFT calculated Gibbs free energy of complexation for Pu^{4+} ion was found to be higher with HONTP than with HONTA. Different bonding analysis indicates the electrostatic and small covalent nature of the interactions between the metal ions and HONTP.

This study clearly demonstrates the effect of one methylene group in the spacer length of a ligand (HONTA *versus* HONTP) on the binding efficiency/selectivity and the complex stoichiometry.

Experimental

Chemicals

The synthesis of HONTA was carried out according to a reported procedure.[29] The diluents isodecanol (SRL, Mumbai) and *n*-dodecane (Lancaster, UK) were used as received. Oxalic acid ($H_2C_2O_4{\cdot}2H_2O$), 3,3′,3″-nitrilotripropionic acid, and 2-thenoyltrifluoroacetone (TTA) were purchased from Fluka (Switzerland), TCI Europe (Belgium) and Sigma-Aldrich (USA), respectively, with purity >99%. Preparation of the dilute nitric acid solutions for the solvent extraction as well as the SLM transport studies was done using Suprapur nitric acid (Merck) and milli Q water (Millipore, USA). All the other chemicals used were of Analytical Reagent grade.

3,3′,3″-Nitrilotris(*N*,*N*-di-*n*-octylpropanamide) (HONTP)

To a solution of 3,3′,3″-nitrilotripropionic acid (0.233 g, 1 mmol, 1 equiv.) and EDCI (0.86 g, 4.5 mmol, 4.5 equiv.) in pyridine (15 mL), was added di-*n*-octylamine (0.795 g, 3.3 mmol, 3.3 equiv.), and the mixture was stirred at 60 °C for 18 h. Pyridine was removed under reduced pressure. Diethyl ether (50 mL) was added to the residue and the resulting solution was

washed with 0.5 M HCl (3 × 50 mL), saturated $NaHCO_3$ (3 × 50 mL), NaCl solution (50 mL), whereupon the organic layer was dried over Na_2SO_4. The solvent was removed by vacuum evaporation and the residue was purified by column chromatography on silica gel (dichloromethane: ethyl acetate = 20 : 1, R_f = 0.3) to afford pure HONTP in 38% yield (0.35 g).

^{1}H NMR (400 MHz, chloroform-d) δ 3.27–3.24 (m, 6H), 3.22–3.18 (m, 6H), 2.84 (t, J = 7.5 Hz, 6H), 2.48 (t, J = 7.5 Hz, 6H), 1.62–1.44 (m, 2H), 1.28–1.24 (m, 60H), 0.89–0.85 (m, 9 H). ^{13}C NMR (101 MHz, $CDCl_3$) δ 171.2, 77.4, 77.0, 76.7, 49.7, 48.0, 45.96, 31.83, 31.80, 30.5, 29.7, 29.4, 29.35, 29.29, 29.27, 29.2, 27.8, 27.1, 27.0, 22.6, 14.1. IR (ν/cm^{-1}) 3683.83, 2957.97, 2921.21, 2854.69, 1640.63, 1460.39, 1424.72, 1373.52, 1270.28, 1255.52, 1176.85, 1136.86, 1119.15, 1048.96, 763.57, 724.93, 482.86. HRMS: m/z calcd for $C_{57}H_{114}N_4O_3$ $(M + H)^+$ 903.8969; found 904.0097.

Membrane support

PTFE (polytetrafluoroethylene) flat sheet membranes (Sartorius, Germany) were used in the transport experiments. The physical parameters of the membrane used in the SLM studies are: pore size: 0.45 μm; porosity: 64%; diameter: 47 mm; thickness: 80 μm. The pore size of the membranes was checked using Hg porosimetry measurements, while the thickness was confirmed using a Mututoya digital micrometer.

Radiotracers

Pu (mainly ^{239}Pu) from the laboratory stock solution was used after purification by TTA[30] as extractant, which separates the Pu from ^{241}Am (a daughter product of ^{241}Pu). Similarly, the laboratory stocks of ^{233}U and ^{241}Am tracers were purified as per reported methods. Details of the purification are given in the ESI.† The concentrations of ^{239}Pu, ^{233}U and ^{241}Am used were 10^{-6} M, 10^{-5} M, and 10^{-7} M, respectively.

Computational methodology

Structures of free HONTA and HONTP and their complexes with Pu^{4+} and UO_2^{2+} ions in presence of nitrate ion were optimized using the Becke–Lee–Young–Parr (B3LYP) density functional[31,32] employing the split-valence plus polarization (SVP) basis set[33] as implemented in the TURBOMOLE suite of program.[34] The scalar relativistic effective core potentials (ECP) were used for both Pu and U, where 60 electrons were kept in the core for Pu and U.[35] Optimization was performed without any symmetry restrictions. The free energy was computed at 298.15 K using the B3LYP functional.[31] The hybrid B3LYP functional was shown to be quite successful in predicting the thermodynamic properties of actinides.[36–39] The solvent phase was accounted for using the popular conductor like screening model (COSMO).[33] The dielectric constant of water and the organic solvent (90% n-dodecane + 10% isodecanol) was taken to be 80 and 3.03, respectively. The Gibbs free energy of complexation for the various complexation reactions was evaluated using the prescription published earlier.[40] Other details of the DFT studies and the coordinates of the optimized structures are given in the ESI.†

Conflicts of interest

There are no conflicts of interest to declare.

Acknowledgements

The computer division, BARC, is acknowledged for providing the Anupam supercomputing facility. SMA sincerely thanks Mr K. T. Shenoy, Director, Chemical Engineering Group, BARC for continuous encouragement.

References

1 G. Choppin and A. Morgenstern, *J. Radioanal. Nucl. Chem.*, 2000, **243**, 45–51.
2 Y. Ban, S. Hotoku, N. Tsutsui, A. Suzuki, Y. Tsubata and T. Matsumura, *Procedia Chem.*, 2016, **21**, 156–161.
3 T. Siddall III, *J. Phys. Chem.*, 1960, **64**, 1863–1866.
4 N. Condamines and C. Musikas, *Solvent Extr. Ion Exch.*, 1992, **10**, 69–100.
5 K. McCann, J. A. Drader and J. C. Braley, *Sep. Purif. Rev.*, 2018, **47**, 49–65.
6 G. Casparini and G. Grossi, *Sep. Sci. Technol.*, 1980, **15**, 825–844.
7 K. McCann, B. J. Mincher, N. C. Schmitt and J. C. Braley, *Ind. Eng. Chem. Res.*, 2017, **56**, 6515–6519.
8 D. Prabhu, G. Mahajan and G. Nair, *J. Radioanal. Nucl. Chem.*, 1997, **224**, 113–117.
9 G. Nair, G. Mahajan and D. Prabhu, *J. Radioanal. Nucl. Chem.*, 1995, **191**, 323–330.
10 Y. Ban, H. Suzuki, S. Hotoku, N. Tsutsui, Y. Tsubata and T. Matsumura, *Solvent Extr. Ion Exch.*, 2019, **37**, 489–499.
11 Y. Sasaki, Y. Sugo, S. Suzuki and S. Tachimori, *Solvent Extr. Ion Exch.*, 2001, **19**, 91–103.
12 A. Karak, B. Mahanty, P. K. Mohapatra, R. J. M. Egberink, T. Valsala, D. Sathe, R. Bhatt, J. Huskens and W. Verboom, *Solvent Extr. Ion Exch.*, 2022, **40**, 366–386.
13 B. Mahanty, A. Karak, P. K. Mohapatra, R. J. M. Egberink, T. P. Valsala, D. B. Sathe, R. B. Bhatt, J. Huskens and W. Verboom, *Chem. Eng. Process.*, 2021, **161**, 108323.
14 A. Karak, B. Mahanty, P. K. Mohapatra, R. J. M. Egberink, T. P. Valsala, D. B. Sathe, R. B. Bhatt, J. Huskens and W. Verboom, *Sep. Purif. Technol.*, 2021, **279**, 119584.
15 A. Karak, B. Mahanty, P. K. Mohapatra, R. J. M. Egberink, T. P. Valsala, D. B. Sathe, R. B. Bhatt, J. Huskens and W. Verboom, *Sep. Sci. Technol.*, 2022, 1–12.
16 P. Mohapatra, M. Iqbal, D. Raut, W. Verboom, J. Huskens and V. Manchanda, *J. Membr. Sci.*, 2011, **375**, 141–149.
17 B. Mahanty, S. A. Ansari, P. K. Mohapatra, A. Leoncini, J. Huskens and W. Verboom, *J. Hazard. Mater.*, 2018, **347**, 478–485.
18 L. J. Bartolotti and K. Flurchick, *Rev. Comput. Chem.*, 2009, **7**, 187–216.
19 C. Wagner, U. Müllich, A. Geist and P. J. Panak, *Solvent Extr. Ion Exch.*, 2016, **34**, 103–113.
20 G. R. Choppin and K. L. Nash, *Radiochim. Acta*, 1995, **70**, 225–236.

21 R. D. Shannon, *Acta Crystallogr., Sect. A: Cryst. Phys., Diffr., Theor. Gen. Crystallogr.*, 1976, **32**, 751–767.
22 A. Sengupta and M. Murali, *Sep. Sci. Technol.*, 2016, **51**, 2153–2163.
23 M. Basu, P. Sinharoy, J. Ramkumar, S. L. Gawali, B. Dutta and J. Sharma, *J. Solution Chem.*, 2019, **48**, 1318–1335.
24 P. Pathak, L. Kumbhare and V. Manchanda, *Radiochim. Acta*, 2001, **89**, 447–452.
25 R. B. Gujar, P. K. Mohapatra and W. Verboom, *Sep. Purif. Technol.*, 2020, **247**, 116986.
26 P. Verma, P. Mohapatra, A. Bhattacharyya, A. Yadav, S. Jha and D. Bhattacharyya, *New J. Chem.*, 2018, **42**, 5243–5255.
27 A. E. Reed and F. Weinhold, *J. Chem. Phys.*, 1983, **78**, 4066–4073.
28 A. E. Reed, L. A. Curtiss and F. Weinhold, *Chem. Rev.*, 1988, **88**, 899–926.
29 A. Bhattacharyya, P. K. Mohapatra, A. S. Kanekar, K. Dai, R. J. M. Egberink, J. Huskens and W. Verboom, *ChemistrySelect*, 2020, **5**, 3374–3384.
30 M. Sajun, V. Ramakrishna and S. Patil, *Thermochim. Acta*, 1981, **47**, 277–286.
31 D. B. Axel, *J. Chem. Phys.*, 1993, **98**, 5648–5652.
32 C. Lee, W. Yang and R. G. Parr, *Phys. Rev. B: Condens. Matter Mater. Phys.*, 1988, **37**, 785.
33 A. Schäfer, H. Horn and R. Ahlrichs, *J. Chem. Phys.*, 1992, **97**, 2571–2577.
34 R. Ahlrichs, M. Bär, M. Häser, H. Horn and C. Kölmel, *Chem. Phys. Lett.*, 1989, **162**, 165–169.
35 X. Cao and M. Dolg, *J. Mol. Struct. THEOCHEM*, 2004, **673**, 203–209.
36 G. A. Shamov, G. Schreckenbach and T. N. Vo, *Chem. – Eur. J.*, 2007, **13**, 4932–4947.
37 S. Pahan, A. Boda and S. M. Ali, *Theor. Chem. Acc.*, 2015, **134**, 1–16.
38 S. M. Ali, S. Pahan, A. Bhattacharyya and P. Mohapatra, *Phys. Chem. Chem. Phys.*, 2016, **18**, 9816–9828.
39 A. S. Deb, S. M. Ali and K. Shenoy, *RSC Adv.*, 2015, **5**, 80076–80088.
40 A. Klamt, *J. Chem. Phys.*, 1995, **99**, 2224–2235.

